

Application of a distributed GIS model for studying surface runoff processes in an urban wetland

J. Chormanski^{1*}, O. Batelaan¹, F. De Smedt¹, T. Van de Voorde², F. Canters²

1. Department of Hydrology and Hydraulic Engineering, Vrije Universiteit Brussel, Brussels, Belgium

2. Department of Geography, Vrije Universiteit Brussel, Brussels, Belgium

*currently: Department of Hydraulic Structures and Environmental Restoration, Warsaw Agricultural University, Warsaw, Poland

ABSTRACT: The Woluwe is a small river that drains an area of 9400 hectares in the Belgian part of the Scheldt basin. The central part of the Woluwe River flows partially through several park and pond systems of the Brussels agglomeration. Within the Woluwe catchment there are drinking water wells, wetlands in seepage zones and 21 ponds with different functions (water storage, fish-stock, recreational fishing, boating, ornamental parks, wetland, nature value). In urban catchments, surface runoff is the most important process that determines the water quantity and quality. An analysis of potential differences in runoff generation, influenced by land-use changes in the catchment, could provide information on the future hydrological state of the urban wetlands. Similarly, an evaluation of the runoff partitions from different land-uses could show the possible source of water pollution in urban wetlands. A distributed modelling approach, on basis of the WetSpa model and supported by remotely sensed data, was used for studying runoff in the Upper Woluwe catchment. WetSpa is a GIS grid-based distributed hydrological model that simulate with an hourly time step peak discharges, hydrographs and the spatial distribution of runoff, infiltration and evapotranspiration. The WetSpa model is applied to analyze the effects of topography, soil type, and land-use on the flood characteristics. More specifically, the assessment of imperviousness estimated on basis of remote sensing and its influences on runoff generation are described.

1 INTRODUCTION

Urban areas are a cover type, which is difficult to parameterize in hydrological modeling, mainly due to the fact that urban areas are not homogeneous. Surface imperviousness is a predominant pattern of various urban cover types. One of the most obvious effects of urban growth is an increase of impervious surface cover. Surface imperviousness has been identified as a key factor of flash floods, which are in general increasingly observed in the last century. Another problem in urban areas is the difficulty to separate impervious surfaces from different pervious land-use types (grass, trees, bare soils,...). This is mostly the result of a map generalization process, in which the generalization level depends on the map scale, e.g. build-up areas also contain gardens and vegetation. Some urban classes are by definition not homogenous, such as “open build-up”, which mostly refers to residential areas or parks where the degree of imperviousness is rather small and randomly distributed over the whole class. Usually, there is no information concerning the degree of imperviousness of different urban classes. Hence, these values have to be estimated for the purpose of hydrological modeling. This paper presents how an existing land-use

map could be improved by high resolution (Landsat ETM+) and very high resolution (Ikonos VHR) remotely sensed data, and how this influences the runoff generation. The WetSpa distributed hydrological model is applied for flood prediction and used to analyze the influence of impervious area estimations on peak flow. Different methods to assess or calculate the degree of imperviousness, with and without remote sensing information, are analyzed in different runoff simulation scenarios.

2 METHOD

2.1 Introduction

Since physically based distributed hydrological modeling on catchment scale requires many input layers and generate spatially distributed outputs, GIS is a very useful tool because of its efficiency in data storage, display and maintenance. In addition to the today's development of improved computational capabilities, Digital Elevation Model (DEM), digital data of soil type and land-use, as well as the powerful GIS tools give new possibilities for hydrological

research in understanding the fundamental physical processes underlying the hydrological cycle and the solution of mathematical equations representing those processes. Recently, many hydrological models with a flood prediction component have been developed or updated to use DEM's, such as the model SWAT (Arnold et al., 1998), CASC2D (Downer et al., 2002), DWSM (Borah et al., 2002), HYDROTEL (Fortin et al., 2000), whereas models like SHE and TOPMODEL were adapted to benefit from GIS data (Quinn et al., 1991; Ewen et al., 2001). These models are either loosely or tightly coupled with GIS and remotely sensed data. Olivera & Maidment (1999) proposed a method for routing spatially distributed excess precipitation over a watershed using response functions derived from a digital terrain model, in which the routing of water from one cell to the next is accomplished by using the first-passage-time response function derived from the advection-dispersion equation. The flow path response function is calculated by a convolution integral of the cell response functions along the flow path, which makes it possible to route excess rainfall from each grid cell to the basin outlet. Increasingly GIS technology and remote sensing is integrated with hydrological modeling, while making use of DEM availability flood prediction with these distributed models tends to be more advantageous.

2.2 Model

WetSpa is a grid-based distributed hydrological model for water and energy transfer between soil, plants and atmosphere, which was originally developed by Wang et al. (1996) and adopted for flood prediction on hourly time step by De Smedt et al. (2000), and Liu et al. (2002). For each grid cell a vegetation, root, transmission and saturated zone is considered in the vertical direction. The hydrological processes parametrised in the model are: precipitation, interception, depression, surface runoff, infiltration, evapotranspiration, percolation, interflow and groundwater flow. The total water balance for a raster cell is composed of the water balance for the vegetated, bare-soil, open water and impervious parts of each cell. This allows accounting for the non-uniformity of the land-use per cell, which is dependent on the resolution of the grid. A mixture of physical and empirical relationships is used to describe the hydrological processes in the model. Interception reduces the precipitation in net precipitation, which on the ground is separated into rainfall excess and infiltration. Rainfall excess is calculated using a moisture-related modified rational method with a potential runoff coefficient depending on the land-cover, soil type, slope, magnitude of rainfall, and antecedent moisture content of the soil. The calculated rainfall excess fills the depression storage at the initial stage and runs off the land surface simul-

taneously as overland flow (Linsley, 1982). The infiltrated part of the rainfall may stay as soil moisture in the root zone, move laterally as interflow or percolate as groundwater recharge depending on the moisture content of the soil. Both percolation and interflow are assumed to be gravity driven in the model. Percolation out of the root zone is determined by the hydraulic conductivity, which is dependent on the moisture content as a function of the soil pore size distribution index. Interflow is assumed to occur in the root zone after percolation and becomes significant only when the soil moisture is higher than field capacity. Darcy's law and a kinematic approximation are used to estimate the amount of interflow generated from each cell, in function of hydraulic conductivity, moisture content, slope, and root depth. The actual evapotranspiration from soil and plant is calculated for each grid cell using the relationship developed by Thornthwaite & Mather (1955) as a function of potential evapotranspiration, vegetation stage, and moisture content in the cell.

Runoff from different cells in the watershed is routed to the watershed outlet depending on flow velocity and wave damping coefficient by using the diffusive wave approximation method. An approximate solution proposed by De Smedt et al. (2000) in the form of an instantaneous unit hydrograph (IUH) was used in the model, relating the discharge at the end of a flow path to the available runoff at the start of the flow path

$$U(t) = \frac{1}{\sigma \sqrt{2\pi^3/t_0^3}} \exp\left[-\frac{(t-t_0)^2}{2\sigma^2 t/t_0}\right] \quad (1)$$

where $U(t)$ [T^{-1}] is the flow path unit response function, t_0 [T] is the mean flow time, and σ [T] is the standard deviation of the flow time. Parameters t_0 and σ are spatially distributed, and can be obtained by integration along the topographic determined flow paths as a function of flow celerity and dispersion. Although the spatial variability of land-use, soil and topographic properties within a watershed are considered in the model, the groundwater response is modeled on sub-catchment scale. The simple concept of a linear reservoir is used to estimate groundwater discharge, while a non-linear reservoir method is optional in the model (Wittenberg & Sivapalan, 1999). The groundwater outflow is added to the generated runoff to produce the total streamflow at the sub-watershed outlet. The time-dependent inputs to the model are precipitation and potential evapotranspiration. Model parameters such as interception and depression storage capacity, potential runoff coefficient, overland roughness coefficient, root depth, soil property parameters, average travel time to the outlet, dispersion coefficient, etc., are determined for each grid cell using ArcView lookup tables and high resolution DEM, soil type and land-use maps, or a combination of these maps. The main outputs of the model are river flow hydro-

graphs, which can be defined for any location in the channel network, and spatially distributed hydrological characteristics, such as soil moisture, infiltration rates, groundwater recharge, surface water retention, runoff, etc.

3 RESEARCH AREA

The Woluwe is a small river and is part of the Scheldt basin. The upper part of the catchment up to the Goubert gauge was selected as a study area (Figure 1). The upstream part of this area lies in the protected area of the Sonian forest (South-West of the Brussels District). In the downstream part, the River Woluwe flows partially through several vaulted stretches and park and pond systems (flow-through and overflows). The Upper Woluwe catchment comprises approximately 31 km². The elevation of the catchment ranges from 49 to 129 m, with an average of 94 m above the sea level. The ground elevation increases gradually from the north to the south, with slopes varying between 0 and 22 %, and an average of 6 %. According to the Royal Meteorological Institute at Ukkel, located close to the catchment border, the long-term yearly precipitation is 780 mm/year, the winter precipitation is 380 and summer is 400 mm/year. The long-term open-water potential evaporation of Ukkel is 657 mm/year, the winter potential evaporation is 114 and summer is 543 mm/year. The average temperature is 5.0°C for the winter season and 14.1°C for the summer season. The Woluwe catchment consists for 96 % of the area of loam soils, while the remaining 4 % are occupied by sandy loam soils. The land-use types in the study area are deciduous forest (55 %), urban area (29 %), pine forest (16 %), mixed forests (10 %), agriculture, meadows, wetlands and open water (0.5 %).



Figure 1 Location of the Upper Woluwe Catchment

4 DATA

4.1 Hydrometeorological data

The water stages and discharges are continuously measured since April 2005 in 15 minutes time interval by using ultrasonic method for the two gauges Middlebourg and Hector Goubert. Rainfall with 10 minutes time interval and daily potential evapotranspiration (PET) data are obtained from the Ukkel meteorological station. For the purpose of modelling, the hydrometeorological data are transformed to an hourly time step.

4.2 Spatial data

Three different raster land-use maps were used for runoff simulation: digital Flemish land-use map produced by OC GIS-Vlaanderen, Ikonos VHR (Very High Resolution) image and sub-pixel classified Landsat ETM+ (Enhanced Thematic Mapper). The different land-use datasets have different pixel size (Flemish land-use map - 20 m, Ikonos - 1 m, Landsat - 30 m), hence for modelling purposes the maps were resampled to the lowest resolution, 30 m. A DEM with 30 times 30 m grid resolution was constructed from elevation contours and the official river network. The elevation contours for every 2.5 m were obtained from topographic maps with a scale 1:10,000. The DEM was generated in ArcInfo using TOPOGRID (Hutchinson, 1989), which is a very useful tool for reliable generation and error correction of a DEM with limited elevation data based on contours and point elevation information (Wise, 2000). A soil map has been obtained from OC GIS-Vlaanderen in digital form and converted to 12 USDA soil texture classes based on textural properties.

5 REMOTE SENSING METHOD

Generally speaking, the remote sensing approach involves two steps. First, a detailed land-cover map is produced from very high resolution (VHR) imagery covering part of the study area. The enhanced VHR classification is then used to train a neural network sub-pixel classification model that estimates impervious surface cover proportions within the pixels of a high-resolution (HR) image covering a much larger area.

5.1 Developing the reference land-cover classification

We used an ANN to build the reference land-cover classification, which consists of 11 classes: light and dark red surfaces, light, medium and dark grey sur-

faces, bare soil, water, crops, shrub and trees, grass, and shadows. This neural network was created with Neuralware's NeuralWorks Predict® software. The accuracy of the resulting land-cover map was assessed with independent validation data.

Training data for this classification were obtained by digitizing about 200 random training pixels per class on the Ikonos image. As an independent validation set, we chose a stratified random sample: the amount of pixels to be sampled in each class depended on the class's prominence in the image. With the training data, neural network models were built according to 4 scenarios. Each type of network had a different combination of input variables: only the multi-spectral bands, the multi-spectral bands with the PAN band, the multi-spectral bands with the PAN band and a vegetation index (NDVI), and the multi-spectral bands with PAN, NDVI and 2 texture measures. The texture measures we used were local variance and binary comparison matrix (Murphy, 1985). Transformations of the input bands and a selection according to their relative contribution to the overall information content were accomplished with NeuralWorks Predict®. The transformed input variables that were retained in each scenario to actually perform the classification were chosen from a set of 5 mathematical transformations per original input band using a genetic-based variable selection algorithm embedded in the software.

The success of our sub-pixel classification strategy depends heavily on obtaining reliable training data, i.e. accurate land-cover proportions for each ETM+ training pixel. Because many potential sources of bias were present in the resulting land-cover map, we improved its accuracy and coherence with several post classification techniques: shadow removal, structural filtering (Barr & Barnsley, 2000) and correction of classification errors with knowledge-based rules. To this end, we adopted the method and workflow suggested by Van de Voorde et al. (2004, 2006). The 11 classes were aggregated afterwards to a single vegetation class (including shrub and trees, grass and crops), a single "impervious surfaces" class (including red and grey surfaces), water class and bare soil class.

5.2 Subpixel classification

Once reliable reference data were obtained, we could build neural network models for sub-pixel classification with a random sample of high resolution pixels, which were drawn from the part of the image that overlaps the VHR classification. Each sample point consisted of the spectral values of the ETM+ pixel and the proportion of the four target classes (bare soil, built-up surfaces, water and vegetation) within this pixel.

Because it will be very difficult in practice to obtain HR and VHR images of the same dates, it is likely

that land-cover changes are present in the images used in a multi-resolution approach. These changes may be seasonal (leaf-on versus leaf-off for deciduous trees, crop cycles) or point to actual land-use changes (e.g. urban growth). To remove changed pixels from the random sample of HR pixels, we assumed that the Normalized Difference Vegetation Index (NDVI) of the HR pixels shows a clear relationship with the average NDVI of the constituent VHR pixels and applied a non-linear regression to remove outlying pixels. In doing so, we had to take into account that the digital numbers (DN), which represent the spectral response from the visible red and near infrared channels required to calculate NDVI, originate from two different sensor platforms. To account for this, they were converted to in-band radiance at sensor aperture. This was achieved with the equations proposed by Taylor (2005) for the Ikonos images and by Irish (2000) for the ETM+ image.

Two models were then built with NeuralWare's Predict software and compared independently. These models differed in the type of input variables, i.e. spectral channels that were used. The first model had the six ETM+ multispectral bands as input (bands 1-5 and band 7). The second model included all possible ratios between the spectral channels in addition to the multispectral channels. The performance of the models was assessed by applying them on an independent validation set to estimate the proportions of each of the four classes (Van de Voorde, 2006).

5.3 Preparing data for hydrological modeling

For the purpose of hydrological modeling, the VHR classification was aggregated to a resolution of 30 meters. During aggregation, the proportions of the class's impervious surfaces, water, vegetation (with subclasses meadow, crops and trees) and bare soil were calculated for every aggregated pixel. With the sub-pixel approach, the proportions of the same 4 classes are estimated for each Landsat ETM+ pixel, which also measures 30 by 30 meters. This provides us with two datasets of 30 meter resolution, which are both used to derive the degree of imperviousness used for the runoff simulation scenarios.

6 APPLICATION

6.1 Model calibration

The spatial distribution of the parameters are calculated based on digital maps of elevation, soils, land-use, and field measurements of hydraulic properties of the river channel. Global parameters were adjusted during trial and error calibration procedure, which consisted of running the model as many times

as needed to adjust until the discrepancies between model outputs and observations were satisfactory. The model was evaluated by graphical comparison of simulated and observed hydrographs. Due to the quality of runoff data, the calibration was limited to the global model parameters, whereas the spatial model parameters were kept constant.

6.2 Formulation of scenarios

Using satellite imagery we can improve the land-use data by estimation of an average impervious percentage for urban area (scenario 1, in case of one non-distributed urban class), an average impervious percentage for different classes of urban area (scenario 2, in case of knowledge about various class distribution of urban area), and an percentage of imperviousness for every cell (scenario 3). Accordingly, the different simulation scenarios were elaborated.

6.2.1 Scenario 1: Non-distributed percentage of the surface imperviousness

This scenario assumes one type of city class with an average percentage of imperviousness for the whole urban area. It simulates a situation, which occurs regular in practical hydrology: there is no information about neither urban type nor percentage of impervious distribution. The urban classes from the Flemish land-use map were reclassified to WetSpa codes assuming one class for every urban cover type. Next, according to the WetSpa default values, 30% of urban area was treated as impervious and the remaining as grass. For this combination the surface runoff coefficient and depression storage are calculated as a weighted average (Liu & De Smedt, 2005). This basic scenario was improved by using remote sensing data applied to estimate the average percentage of imperviousness in the urban area.

6.2.2 Scenario 2: Semi-distributed percentage of surface imperviousness

In this scenario, each urban class has a unique Manning coefficient and a constant percentage of imperviousness (Table 1). The land-use map of Flanders with original cover types was used for the urban area. The Manning coefficient has been parameterized as proposed by Van der Sande et al. (2003) and Chow (1959). Three categories of imperviousness are distinguished: 30% for residential area, which was assumed to be same as for the class *open build-up* area, 70% for *city centre* and *industrial* and 50% for *infrastructure* and *build-up* urban classes (Liu, 2004), and also 50% for the class *roads and highways*. The remaining of the urban cells is treated as grass, consequently the surface runoff coefficient and depression storage are calculated as weighted averages. This semi-distributed scenario was improved by use remote sensing data. The average im-

pervious percentage is estimated for the different classes of urban area in two variants; firstly using Ikonos aggregated data and secondly using Landsat imagery with sub-pixel classification.

6.2.3 Scenario 3 Fully-distributed percentage of surface imperviousness

In this scenario a fully-distributed assignment of the impervious percentage in the urban area is used. The land-use in every urban cell is described as the sum of the percentages of the cover types impervious, bare soil, vegetation and water. The runoff coefficient and depression storage are estimated as an area weighted average of the parameters for *impervious*, *bare soil*, *vegetation* and *water*. The Manning coefficient is constant for every urban cell and has the same value as in scenario 1.

6.3 Results

6.3.1 Scenario 1

The results of the imperviousness classification were very similar for both data sources, respectively 44% for Ikonos VHR data and 46% for the Landsat sub-pixel classified image. The simulated hydrographs for the 30% (default) and 44% imperviousness scenario (Ikonos improvement) shows, that the remote sensing data are a valuable source for improving runoff calculation with only one type of city class with an average impervious percentage. The simulated discharge peaks are 10-20% higher in the scenario with Ikonos data. Hence, significant differences are observed in the hydrographs (Figure 2).

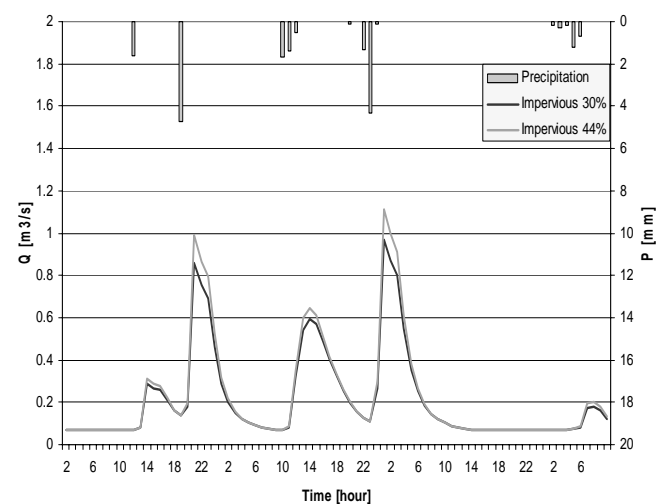


Figure 2 Hydrographs for scenario 1 with 30% (default) and the 44% imperviousness (Ikonos improvement) for the period 3rd of May 2005 1.00 am till 6th of May 2005 9.00 am.

6.3.2 Scenario 2

The results of scenario 2 are shown in Table 1. It is noticed that the impervious percentages estimated on basis of different remote sensing data sources are similar. However, the on remote sensing based im-

perviousness for the *open build-up* and *city centre* class is much smaller than the default assumed imperviousness. Very good agreement is found in estimated and default values for *infrastructure* and *build-up*, as well as for the *industrial* class. In these classes estimated values were always higher than the default. For the class of *road and highways* the remote sensing estimated imperviousness was smaller than the default assumed imperviousness. These relatively large differences in percentage of impervious areas appear to have no big influence on the simulated hydrograph. The runoff hydrograph simulated based on the average imperviousness determined by remote sensing is slightly higher than the one determined with semi-distributed default values (Figure 2). In the beginning of the test period a relatively big difference is observed between the simulated peak discharge for scenario 1 and 2. Also a one hour shift of peak flow is observed for high rain intensities compared to scenario 1 (Figure 3). These effects can be explained by differences in manning coefficient, and their influence on the results. An increase of the runoff coefficient is observed in urban area located close to the river outlet in the north of the catchment and a decrease in areas located relatively far from the outlet.

Table 1 Manning roughness coefficients and impervious percentage values per different urban classes: default and estimated based on different remote sensing data

Cover type	Manning coeff.	Default assumed % impervious	Estimated % impervious		Area of cover type [km ²]
			Aggregation from Ikonos	Landsat	
<i>Resident/open build-up</i>	0.2	0.30	0.12	0.12	2.54
<i>Build-up /pavements</i>	0.05	0.50	0.57	0.61	3.94
<i>City centre build-up</i>	0.05	0.70	0.45	0.38	0.19
<i>Infrastructure</i>	0.05	0.50	0.58	0.60	1.73
<i>Road/Highway</i>	0.01	0.50	0.36	0.31	0.58
<i>Industrial/Agency</i>	0.2	0.70	0.84	0.86	0.14

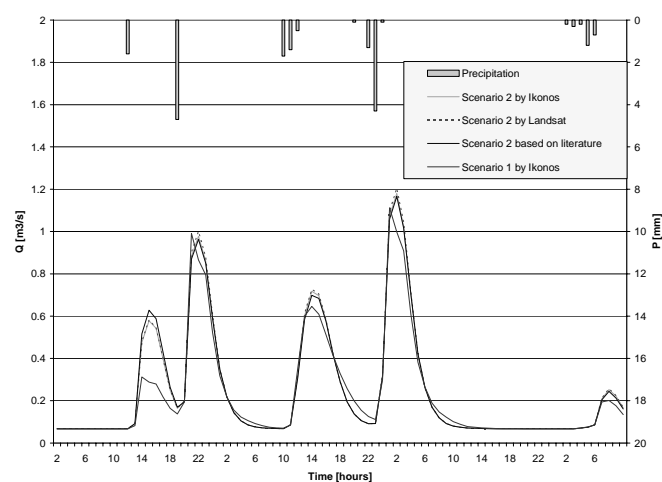


Figure 3 Comparison of hydrographs resulting from semi-distributed urban class scenarios for the period 3rd of May 2005 1.00 am till 6th of May 2005 9.00 am.

6.3.3 Scenario 3

In scenario 3 hydrographs are simulated for the fully-distributed imperviousness based on Ikonos HRV and Landsat sub-pixel classified images. Results are compared to the simulated hydrograph of scenario 1, which is improved by use of Ikonos data. Analysing the results we observe that the runoff calculated in Scenario 3 and based on Ikonos data gives the highest discharges. The maximum peaks are about 10% higher than simulated in scenario 1 on basis of Ikonos data. This proves that for runoff simulation it is essential to know what the impervious percentage in urban area is, but even more important is to analyse its spatial distribution. Hence, including distributed imperviousness in runoff simulation can strongly improve flood prediction. This advantage is only possible when using a fully-distributed grid based hydrologic model. The hydrograph simulated in scenario 3 and based on Landsat data is slightly lower than simulated in scenario 3 and based on Ikonos data. However, the Landsat dataset is advantageous for runoff simulation, considering its low cost and the larger area it covers compared to Ikonos data. The spatial differences in runoff are obvious from the map of runoff coefficients based on Ikonos data (Figure 4). High values of runoff coefficients, in the range of 0.8-1.0, are observed at some isolated locations. Runoff occurring in these areas has little impact on the hydrograph due to the moderating effect of neighbouring areas with lower runoff coefficients. Hence, the connectivity between cells becomes a very important factor influencing the discharge volume. Figure 4 presents a comparison of simulated hydrographs for all scenarios of imperviousness distribution elaborated in this study: Scenario 1 with a non-distributed default average imperviousness percentage of 30%; Scenario 1 with a non-distributed average imperviousness percentage of 44% estimated from Ikonos; Sce-

nario 2 with a semi-distributed imperviousness percentage for different classes estimated from Ikonos and Scenario 3 with a fully-distributed imperviousness percentage. Simulated hydrographs show a relation between the type of impervious area distribution and simulated runoff. The highest discharges are always calculated for the fully-distributed scenarios, and the lowest for non-distributed ones. The scenarios as presented in the order of Figure 5 show an increased connectivity of urban impervious areas. This connectivity is the main cause of the increase in simulated discharge for scenario 1 to 3.

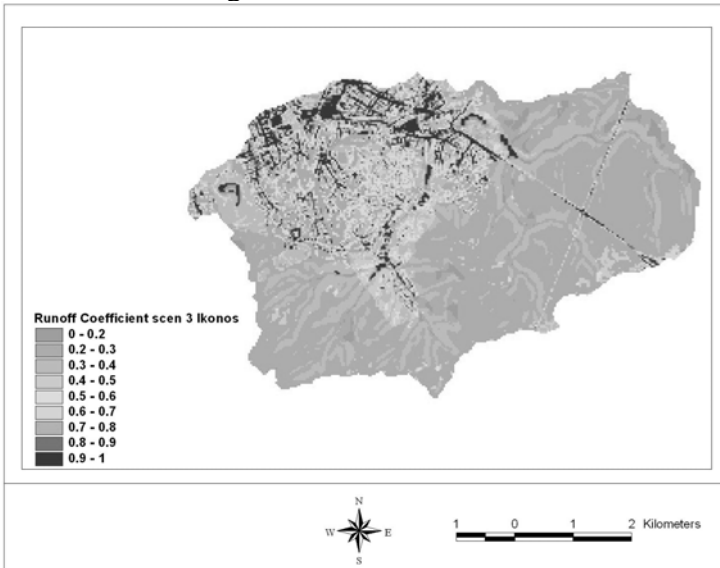


Figure 4 Map of runoff coefficients obtained in scenario 3 with fully-distributed impervious percentage estimated on basis of Ikonos data

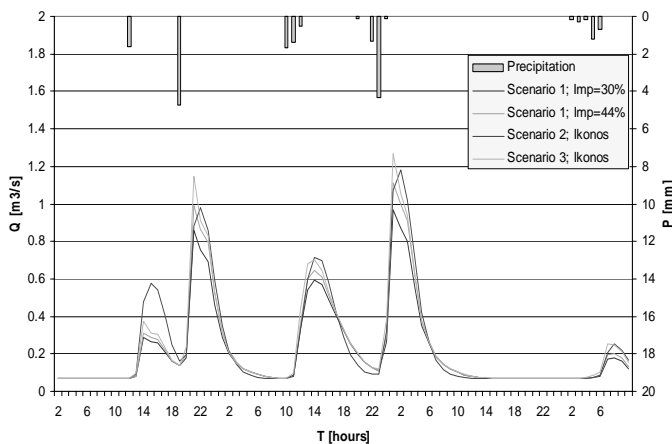


Figure 5 Comparison of hydrographs simulated for 3 scenarios by using Ikonos data. Simulation period 3rd of May 2005 1.00 am till 6th of May 2005 9.00 am.

7 CONCLUSIONS

The WetSpa model, a GIS-based distributed hydrological model, was successfully applied for the Upper Woluwe catchment. The WetSpa model approach allows the use of spatially distributed hydrological parameters of the terrain as inputs to the model, and hence enables the analyses of the effects of land-use on the hydrologic behaviour of urban basins. Different scenarios focused on various

methods of impervious surface estimation in urban area, assuming a homogeneous distribution of impervious surfaces at the level of the entire urban area, or at the level of each urban land-use class or at the level of the individual pixel. These analyses lead to the following conclusions:

1. Generally speaking, both tested remote sensing datasets, a multispectral Landsat ETM+ (HR) image and an Ikonos (VHR) image, proved to be very valuable sources for estimating the average percentage of imperviousness in the urban area.
2. Estimation of impervious surface percentage of the urban areas using VHR and HR results in similar predictions. However, HR images are much cheaper and therefore can be recommended as a useful and economical alternative to expensive VHR data for runoff simulation.
3. The use of remote sensing data improves the results of simulation in every scenario.
4. The highest discharges are always obtained with the fully-distributed scenario, the lowest with the non-distributed scenario. More detailed information about the spatial distribution of imperviousness leads to higher simulated discharges.
5. During runoff simulation for the Upper Woluwe catchment the spatial distribution of impervious surfaces proved to be very important. Including distributed information on surface imperviousness in the modeling may strongly improve flood prediction. This, of course, is only possible when a fully-distributed grid-based hydrological model is used.

REFERENCES

- Arnold, J. G., Srinivasan, S., Muttiah, R. S. & Williams, J. R., 1998. Large area hydrologic modeling and assessment, Part I: Model development, *Journal of the American Water Resources Association*, 34(1), 73-87.
- Barr, S.L. & M.J. Barnsley, 2000. Reducing structural clutter in land cover classifications of high spatial resolution remotely-sensed images for urban land use mapping. *Computers and Geosciences*, 26(4): 433-449
- Borah, D.K., Xia, R. & Bera M., 2002. DWSM - A dynamic watershed simulation model, In: *Mathematical Models of Small Watershed Hydrology and Applications*, Ed. Singh V.P. and Freyert D.K., pp. 113-166, Water Resources Publications, LLC, Highlands Ranch, Colorado, USA.
- Chow, V.T., 1959. *Open-Channel Hydraulics*, ISBN 0-07010810-2. McGrawHill, New York, 572 pp.
- De Smedt, F., Liu, Y.B. & Gebremeskel, S., 2000. Hydrologic modeling on a catchment scale using GIS and remote sensed land use information, In: *Risk Analysis II*, Ed. C.A. Brebbia, WTI press, Southampton, Boston, pp. 295-304.
- Downer, C.W., Ogen, F.L., Martin, W. & Harmon, R.S., 2002. Theory, development, and applicability of the surface

- water hydrologic model CASC2D, *Hydrol. Process*, 16(2), 255-275.
- Ewen, J., Parkin, G. & O'Connell, P.E., 2000. SHETRAN: distributed river basin flow and transport modeling system, *J. Hydrologic Eng.*, ASCE, 5, 250-258.
- Fortin, J.P., Turcotte, R., Massicotte, S., Moussa, R., Fitzback, J. & Villeneuve, J.P., 2001. A distributed watershed model compatible with remote sensing and GIS data, I: Description of the model, *J. Hydrological Eng.*, ASCE, 6(2), 91-99.
- Hutchinson M.F. 1989. A new procedure for gridding elevation and stream line data with automatic removal of spurious sinks., *Journal of Hydrology*, 106, 211-232.
- Irish, R. R., 2000. Landsat 7 Science Data Users Handbook, Report 430-15-01-003-0, National Aeronautics and Space Administration, Goddard Space Flight Center, Maryland, URL:http://ftpwww.gsfc.nasa.gov/IAS/handbook/handbook_toc.html (last date accessed: 30 November 2005)
- Linsley, R.K.J., Kohler, M.A. & Paulhus, J.L.H., 1982. *Hydrology for Engineers*, 3rd Ed., McGraw-Hill, New York, p. 237.
- Liu, Y.B., De Smedt, F. & Pfister, L., 2002. Flood prediction with the WetSpa model on catchment scale, In: *Flood Defence '2002*, Ed. Wu et al., Science Press, New York Ltd., pp. 499-507.
- Liu Y.B., 2004. Development and application of a GIS-based hydrological model for flood prediction. Vrije Universiteit Brussel, Belgium, PhD. Thesis pp 315.
- Liu, Y.B. & F. De Smedt, 2005. Flood modeling for complex terrain using GIS and remote sensed information. *Water Resources Management*, 19: 605-624
- Murphy, D.L., 1985. Estimating Neighborhood Variability with a Binary Comparison Matrix. *Photogrammetric Engineering and Remote Sensing*, 51(6):667-674
- Olivera, F. & Maidment, D., 1999. Geographic information systems (GIS)-based spatially distributed model for runoff routing, *Water Resour. Res.*, 35(4), 1155-1164.
- Quinn, P., Beven, K., Chevallier, P. & Planchon, O., 1991. The prediction of hillslope flow paths for distributed hydrological modeling using digital terrain models, *Hydrol. Process*, 5, 59-79.
- Taylor, M., 2005. Ikonos Planetary Reflectance and Mean Solar Exoatmospheric Irradiance, Space Imaging Inc., Thornton, Colorado URL: http://www.spaceimaging.com/whitepapers_pdfs/Esun1.pdf (last date accessed: 30 November 2005)
- Thorntwaite, C. W. & Mather, J. R. 1955. *The water balance*, Laboratory of Climatology, Publ. No. 8, Centerton NJ.
- Van de Voorde, T., W. De Genst, F. Canters, N. Stephenne, E. Wolff & M. Binard, 2004. Extraction of land use/land cover related information from very high resolution data in urban and suburban areas. In: *Remote Sensing in Transition. Proceedings of the 23rd Symposium of the European Association of Remote Sensing Laboratories*, edited by R. Goossens (Millpress, Rotterdam), 237-244
- Van de Voorde, T., W. De Genst & F. Canters, 2006. Improving pixel-based VHR land-cover classifications of urban areas with post-classification techniques. *Photogrammetric Engineering and Remote Sensing*, accepted
- Van Der Sande C.J., de Jong S.M. & A.P.J. de Roo, 2003. A segmentation and classification approach of IKONOS-2 imagery for land cover mapping to assist flood risk and flood damage assessment. *Int. J. of Applied Earth Observation and Geoinformation* 4, 217-229.
- Wang, Z., Batelaan, O. & De Smedt, F., 1996. A distributed model for Water and Energy Transfer between Soil, Plants and Atmosphere, *Phys. Chem. Earth*, 21(3), 189-193.
- Wise S., 2000. Assessing the quality for hydrological applications of digital elevation models derived from contours. *Hydrol. Process*. 14, 1909-1929.
- Wittenberg, H. & Sivapalan, M., 1999. Watershed groundwater balance estimation using streamflow recession analysis and baseflow separation, *J. Hydrol.*, 219, 20-33.